Morphology, Thermal, and Mechanical Properties of Polypropylene/Polyaniline Coated Short Glass Fiber Composites

Rodolfo Cruz-Silva,[1] Jorge Romero-García,[2] Sofía Vazquez-Rodriguez,[2] Jose Luis Angulo-Sánchez[2]

[1]*Centro de Investigación en Ingeniería y Ciencias Aplicadas, UAEM. Av. Universidad 1001, Col. Chamilpa, CP 62210, Cuernavaca, Morelos, México*
[2]*Centro de Investigación en Química Aplicada, Saltillo, Coah. Blvd. Enrique Reyna No. 140, CP 25100 Saltillo, Coahuila, México*

Received 12 June 2006; accepted 14 November 2006
DOI 10.1002/app.26026
Published online 8 May 2007 in Wiley InterScience (www.interscience.wiley.com).

ABSTRACT: Short glass fiber Type E was coated with electrically conducting polyaniline (PAn) by *in situ* chemical polymerization. The resulting PAn coated glass fiber, with surface conductivity of 3.3×10^{-1} S/cm, was melt-compounded with isotactic polypropylene (iPP). Polypropylene grafted with maleic anhydride was investigated as an adhesion promoter for these composites. Differential scanning calorimeter and polarized light microscopy indicates that the PAn coated glass fiber has a strong nucleating activity towards iPP. Scanning electron microscopy showed the improvement in the wetting and dispersion of the fibers when the adhesion promoter was added, although this also led to fiber encapsulation and lowering the electrical conductivity of the composites. The adhesion promoter greatly improved the Young's modulus of the composites, and a reaction between the maleic anhydride groups of the adhesion promoter and the PAn was proposed. Composites with an electrical conductivity greater than 10^{-9} S/cm were achieved using a 30 wt % of PAn coated glass fiber. © 2007 Wiley Periodicals, Inc. J Appl Polym Sci 105: 2387–2395, 2007

Key words: electrically conductive composites; reinforced composites; nucleating agent; adhesion promotor; maleic anhydride copolymer

INTRODUCTION

Polyaniline (PAn), an intrinsically conductive polymer, has been increasingly employed in the preparation of thermoplastic-based composites for antistatic or electromagnetic shielding applications in the last years.[1–7] The great potential of this polymer in the aforesaid applications is due to its environmental stability, relatively high electrical conductivity and low-cost synthetic route.[8] Compared with traditional electrically conductive metallic fillers, PAn has advantages such as lower weight, lower cost, and higher corrosion resistance. However, PAn is infusible, and direct blending of PAn powder with thermoplastics by melt processing techniques results in incomplete dispersion leading to composites with poor mechanical properties. Since the introduction of counter-ion induced processability,[9] blends of PAn and a wide range of thermoplastics have been prepared by extrusion or injection techniques,[1–7,10] but low interfacial adhesion has led to a decrease in the mechanical properties of the blends. For this reason, incorporation of reinforcements or adhesion promoters to PAn-thermoplastic blends is expected to improve the overall mechanical performance of the resulting composites.

The electrical conductivity of composites of insulating and conducting phases is well described by the percolation theory.[11] When a certain amount of conductive filler is gradually added to an insulating matrix, the conductivity of the composite remains close to that of the matrix, but when the amount of conductive filler is high enough to form a continuum network, a drastic increase in the electrical conductivity is achieved. The fraction of conductive filler at this point is called percolation threshold. Further addition of the conductive filler has a less dramatic impact on electrical conductivity. Not only the concentration but also the shape and aggregation behavior of the particles of the conductive filler have strong influence to lower the percolation threshold.[12,13] Theoretical

Correspondence to: R. Cruz-Silva (rcruzsilva@uaem.mx).
Contract grant sponsor: CONACYT; contract grant number: 46046.
Contract grant sponsor: PROMEP; contract grant number: UAEMOR-PTC-151.

This article is dedicated to the memory of Prof. Jose Luis Angulo-Sanchez.

and experimental studies have shown that particles with aggregation behavior or high aspect ratio, such as fiber or flakes, achieve the percolation threshold at lower volume concentrations.[13,14]

It is expected that PAn-coated fibers can achieve the percolation threshold at relatively low concentration not only because of its high aspect ratio but also due to a phenomenon called *double percolation*, common in composites where the conducting phase is located between two nonconducting phases.[15,16] For instance, Taipalus et al.[1] found that in ternary composites of polypropylene (PP)/glass fiber/PAn, location of PAn at the interface between the fibers and the matrix lowered the percolation threshold due to a double percolation mechanism. Nevertheless, upon PAn incorporation, a decrease in the mechanical properties was observed. When conducting carbon fiber was employed instead of glass fiber, an improvement in electrical conductivity was achieved.[4] In this case, the PAn phase behaved as a ''bridge'' to connect the carbon fibers. A similar behavior was observed in composites of nickel flakes coated with conductive polypyrrole.[17] Recently, glass fiber[2] and mica[6] coated with PAn were used to prepare composites with epoxy resin. In these cases, the PAn-coated particles help to develop a conductive network within the composite. However both composites were prepared in liquid media and the polymerization took place after mixing. In melt processing, it is possible that adhesion of physically adsorbed PAn on reinforcements would not be strong enough to resist the high shear during processing.

Since the work done by Gregory et al.,[18] the surface modification of a wide range of fibers with PAn has been extensively studied.[19–22] Geetha et al.[23] studied different sulfonic acid in the surface modification of glass fibers by *in situ* chemical polymerization. However, grafting of PAn to silicon dioxide surfaces using silane coupling agents bearing aniline moieties was first proposed by Wu et al.[24,25] to improve the adhesion between the inorganic substrate and the PAn. Using a similar approach, Li and Ruckenstein successfully grafted PAn on surface treated glass fiber.[26] However, this material has not been used to prepare fiber reinforced composites by melt processing techniques, and optimization of the surface modification process would be interesting.

The aim of this work was to investigate the mechanical, thermal and electric properties of isotactic polypropylene (iPP)/PAn-coated short glass fiber (SGF) composites. The relation between the morphology and both the mechanical and electrical properties was investigated. A PP–maleic anhydride copolymer, a widely used adhesion promoter in PP/SGF composites,[27] was incorporated to the composites to improve their mechanical properties. In addition, a novel reactor design for PAn coating of SGF by *in situ* polymerization is presented.

EXPERIMENTAL

Materials

Aniline was acquired from Baker (Xalostoc, Mexico) and distilled under reduced pressure before use. SGF Type E was acquired from Vitro Group (Monterrey, Mexico). *N*-phenyl-γ-aminopropyltrimethoxysilane was a commercial product from Sylquest (Y-9669^{TM}). Polypropylene grafted maleic anhydride copolymer (PP-*g*MA) was acquired from Uniroyal Chemical under the tradename of Polybond 3200. The maleic anhydride content was of 1.0% as determined by FTIR spectroscopy.[28] iPP with a MFI of 3.8 and density of 0.9 g/cm^3, was acquired from Indelpro, Basell. All other reagents were of analytical grade and used as received.

Fiber modification

SGF was calcinated in a furnace at 500°C for 3 h to eliminate the sizing and coupling agents, then washed with water and treated with 10 wt % hydrochloric acid solution for 3 h at 60°C to increase the silanol groups concentration on the surface. Afterwards, the fiber was thoroughly washed with distilled water. After drying, silanization was done by immersion in a 0.025 wt % *N*-phenyl-γ-aminopropyltrimethoxysilane solution in methanol during 24 h. Then, the fibers were rinsed with methanol, dried under nitrogen flow, and finally in a vacuum oven for 3 h at 100°C.

Modification of silanized SGF by *in situ* polymerization of aniline was done in a 5-L jacketed reactor (Fig. 1), where 1.5 kg of SGF was packed, and 4 L of HCl 1.0*N* and 20 mL of aniline were added. Nitrogen was bubbled trough the packed fiber during 2 h and maintained during the polymerization. The reaction was initiated by adding 56.4 g of ammonium persulfate dissolved in 250 mL of degassed 1.0*N* hydrochloric acid. The reaction media was unstirred; however the liquid was recirculated through the packed fiber using a peristaltic pump at approximately 180 mL/min. Temperature was kept close to 0°C by recirculating cooling fluid by the jacket. Three hours after the reaction was initiated deep green PAn-coated SGF was obtained. These fibers were treated in a 2.0 wt % solution of sodium carbonate and washed thoroughly with deionized water. The blue color of the fiber at this stage was indicative of dedoping. The PAn-coated SGF was redoped with *p*-toluenesulfonic acid, which unlike chlorine, has been reported to be thermally stable up to 200°C as doping agent.[29] Afterwards the fiber was

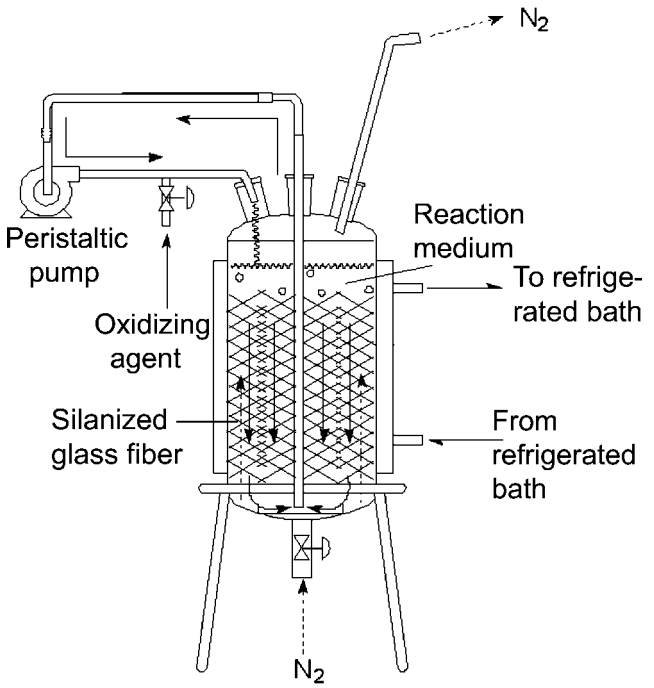

Figure 1 Reactor set up used for short glass fiber (SGF) coating with polyaniline (PAn) by *in situ* chemical polymerization.

dried in a convection oven at 70°C. This procedure afforded PAn-coated SGF, with a fractional PAn weight of 4%, as determined by thermogravimetry. This value indicates that the organic coating is rather a complex of PAn and toluenesulfonic acid in excess; however it will be referred solely as PAn.

Preparation of composites

Prior to mixing, PAn-coated SGF was dried in a vacuum oven for 4 h at 60°C whereas the iPP and PP-*g*MA were dried in a vacuum oven for 12 h at 90°C. Blending was performed in a Banbury Type Mixer at 200°C using CAM rotors. iPP was first melted at 25 rpm for 5 min, PP-*g*MA was added at this point in some formulations. Then, the PAn-coated SGF was added gradually over a 3-min period and mixed for an additional 4-min period. Then the blends were removed from the mixer, cooled to room temperature, and crushed using a mill equipped with a sieve. Finally, the composites were press molded under 2.45 MPa in a steel mold obtaining square composites of 20 cm × 20 cm and 2.6 mm wide.

Characterization

Differential scanning calorimetry

A differential scanning calorimeter (MDSC TA Instruments 2920) was used for thermal analyses. Samples of about 12 mg were loaded in aluminum sealed pans and heated at a rate of 10°C/min from 20 to 200°C, held in this temperature for 3 min to erase previous thermal history, and cooled to room temperature at the same rate and held for 3 min. Then, a second heating scan was performed from 20 to 200°C. The temperatures at the maximum of the crystallization exotherm and the melting endotherm in the second heating scan were taken as the melting (T_m) and crystallization temperatures (T_c), respectively. Calculations of the crystalline fraction of the polymeric phase were done using a heat of fusion of 209 J/g.[30]

Optical and polarized light microscopy

Optical and polarized light microscopy observations of the composites were done in a Olympus BX90 microscope using small samples melted and pressed to form a film. For polarized light microscopy observation, model composites were prepared mixing individual fibers of PAn-coated SGF with melt iPP or PP/PP-*g*MA blends and observed using a Metler-Toledo FP90 heating stage. Samples were heated to 200°C and held in this temperature for 3 min and then cooled to room temperature at 5°C/min.

Mechanical properties

Young's modulus, elongation at break, and tensile strength of the composites were acquired using an Instron universal machine, according to ASTM D638. All samples were cut into dogbones samples and conditioned for 48 h at 51% R.H. and 22°C. The test was run at a 5.08 mm/min deformation rate.

X-ray diffraction pattern

A Siemens D-5000 X-ray diffractometer was used to acquire the wide-angle X-ray diffraction patterns (WAXD) of the press-molded composites. Data acquisition was done in the 2θ mode using a CuKα radiation source (intensity 25 mA, 35 kV acceleration voltage).

Electrical resistance measurements

Single-fiber electrical conductivity measurements were done using a Keithley 2400 sourcemeter. Individual fibers were placed between two silver paint electrodes over a glass slide. The gap between the electrodes was measured by optical microscopy. The electrical resistance of the composites was measured using a Keithley 6517A electrometer/high resistance meter. Samples of 2 cm × 2 cm × 0.26 cm were cut from the compression molded composites, and the insulating skin layer of the composites was carefully removed. Opposite sides of the sample were coated with silver paint to reduce the contact resistance.

The electrical resistance was measured parallel and across the plane of compression. Each value is the average of three measurements.

Scanning electron microscopy

SEM observations were done in a TopCom 510 equipment. Composites samples and PAn-coated SGF were fractured under liquid nitrogen and coated with a thin layer of Au/Pd.

RESULTS AND DISCUSSION

SGF modification and composites formulation

In Figure 2(a) is shown a photo of the PAn-coated SGF after being scratched. This image reveals that the coating is debonded as a free-standing thin film. The inset shows an optical microscopy image of a single fiber that has a uniform coating, as indicated by the homogeneous green color of the fiber. In Figure 2(b), a SEM image of the PAn-coated SGF as obtained after the fiber modification is shown. The morphology of the PAn coating consists of a thin film with particles adhered onto its surface. The thin film is most probably grown from adsorbed aniline on the fibers, whereas the particles are grown in the liquid phase and later adhered on the growing PAn film, in agreement with the growth mechanism of PAn films prepared by *in situ* chemical polymerization.[31] The conductivity of the fiber (3.3×10^{-1} S/cm) is similar to that reported by Li and Ruckenstein,[26] and is high enough to be observed without metallic coating by scanning electron microscopy. Single-fiber conductivity measurements also provided information on the homogeneity of the coating. Electrical conductivity of several fibers from a bundle fluctuates less than one order of magnitude, and less than two orders of magnitude from fibers from a different bundle. By using densities of both materials and the gravimetric results we were able to calculate the average PAn coating thickness ($\sim$ 300 nm) and the electrical conductivity of the bulk

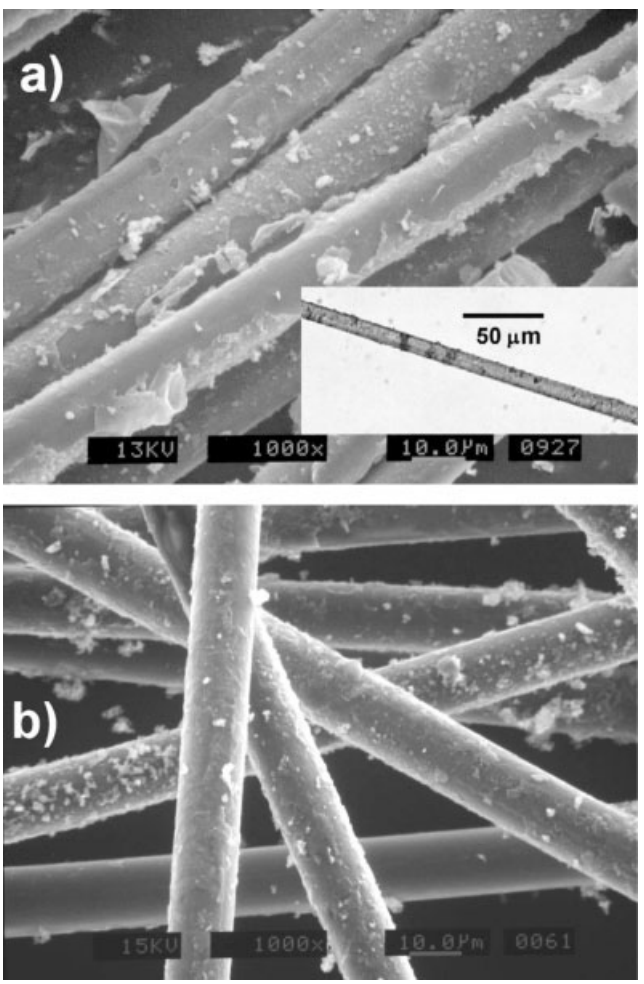

Figure 2 (a) SEM image of PAn coated SGF (PAn-coated SGF) after being scratched. A debonded thin film is observed next to the fiber. The inset shows an optical microscopy image of a single fiber. (b) SEM image of the PAn-coated SGF.

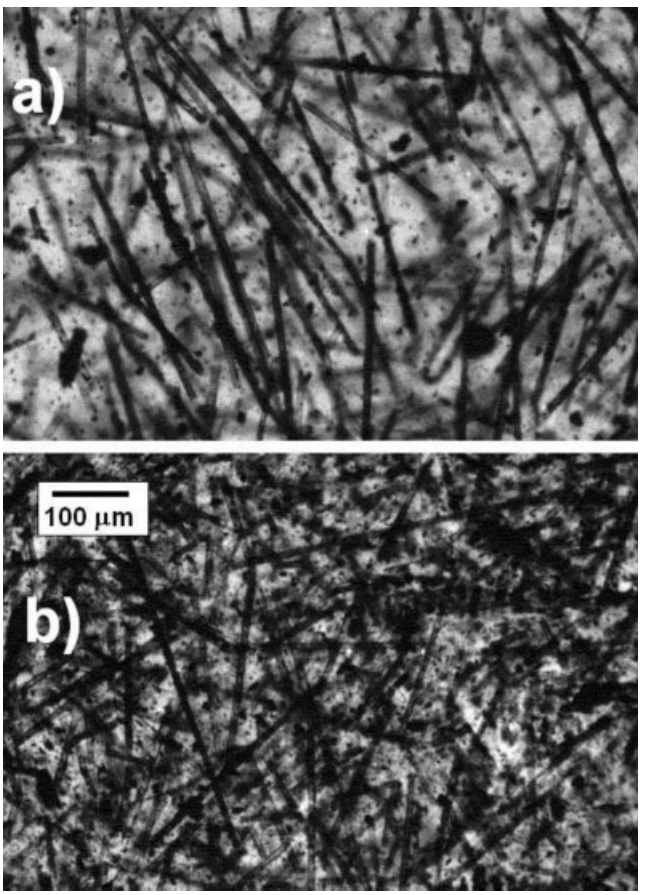

Figure 3 Optical microscopy images of thin films obtained from iPP/PAn-coated SGF composites containing (a) 10 wt % of PAn-coated SGF and (b) 30 wt % of PAn-coated SGF.

PAn of the coating ($\sim$ 3.6 S/cm^{-1}). Optical microscopy images revealed that most of the SGF kept the PAn coating after melt processing at 10 wt % with iPP [Fig. 3(a)]; however, some PAn particles were also present because of debonding of the coating. Increasing the amount of PAn-coated SGF led to a higher degree of debonding, due to fiber abrasion during compounding, but even at 30 wt % of filler load [Fig. 3(b)] a large number of fibers remain coated with PAn.

Effect of the PAn-coated SGF on iPP and iPP/PP-*g*MA crystallization

The effect of the PAn-coated SGF on the thermal properties of iPP and iPP/PP-*g*MA blends was studied by DSC. In Table I, the crystallization temperatures of the composites are shown. The T_c of iPP is 112°C but after the addition of 10 wt % of PAn-coated SGF the T_c increments to 124.2°C. This nucleating activity of PAn-coated SGF towards iPP was previously reported.[32] The thermal properties in presence of the adhesion promoter were also studied. The addition of 5.0 wt % of PP-*g*MA to pure iPP increased the crystallization temperature to 115.7°C. This is attributed to the presence of C=O groups from the maleic anhydride moieties that behave as nucleating points in the nonpolar iPP matrix.[33] The addition of 10 wt % of PAn-coated SGF to the iPP/PP-*g*MA blend increments the T_c to 121.5°C, indicating that the nucleating activity of the PAn is maintained in the presence of PP-*g*MA, contrasting with previous studies on nucleating fibers, where the nucleating activity is suppressed after PP-*g*MA addition to the composite due to fiber encapsulation.[34] Further addition of PAn-coated SGF to the composites causes only a slight increment in the T_c, suggesting that 10 wt % provides enough surface to the polymer matrix to nucleate, and consequently the crystal growth rate becomes limited above that concentration of PAn-coated SGF. The development of transcrystalline zones around PAn-coated SGF in composites, with and without PP-*g*MA, is shown in Figure 4(a,b), respectively. As previously reported, no transcrystallization is induced by the bare glass fiber,[32,33] which is show in Figure 4(c). The width of the crystallization exotherm slightly sharpens in all composites formulations [Fig. 5(a,b)], as compared to the matrix, most likely due to the nucleating effect of the PAn-coated SGF. The crystalline fraction (Table I) slightly increments for the composites as the content of PAn-coated SGF does, indicating that transcrystallization propagate to the matrix.

TABLE I
Composition and Thermal Properties of the Composites

	Composition (wt %)					
Sample	iPP	PP-*g*MA	PAn-coated SGF	T_c	X_c	T_m
PP0000	100	0	0	112.2	0.45	164.8
PP0010	90	0	10	122.4	0.47	164.9
PP0020	80	0	20	123.6	0.49	165.1
PP0030	70	0	30	123.9	0.51	164.6
PP0500	95	5	0	115.7	0.46	164.1
PP0510	85	5	10	121.5	0.47	164.7
PP0520	75	5	20	123.5	0.49	164.9
PP0530	65	5	30	124.6	0.48	164.3

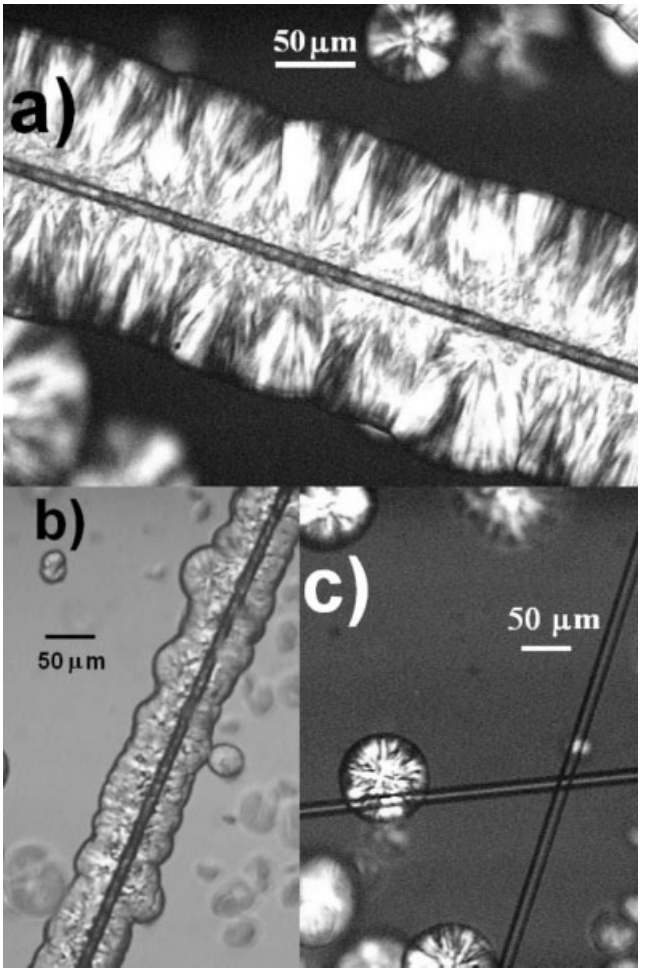

Figure 4 Polarized optical microscopy showing morphology of single PAn-coated SGF embedded in (a) iPP and (b) iPP/PP-*g*MA blend. A single uncoated glass fiber embedded in iPP during crystallization is shown in (c) for comparison.

Surface treatment of SGF and some polymeric fibers can induce transcrystalline zones of different crystal type, such as the γ or β form.[35,36] For this reason, we carried out a study of the composites by wide angle X-ray diffraction, shown in the Figure 6. Nevertheless, the iPP and iPP/PP-*g*MA blend (Fig. 6, curves a and b, respectively), as well as the composites, showed only the characteristic peaks of α-type PP. These peaks appear at 2θ of 14.1°, 16.9°, 18.5°, 21.1°, and 21.8°, and correspond to the (110), (040),

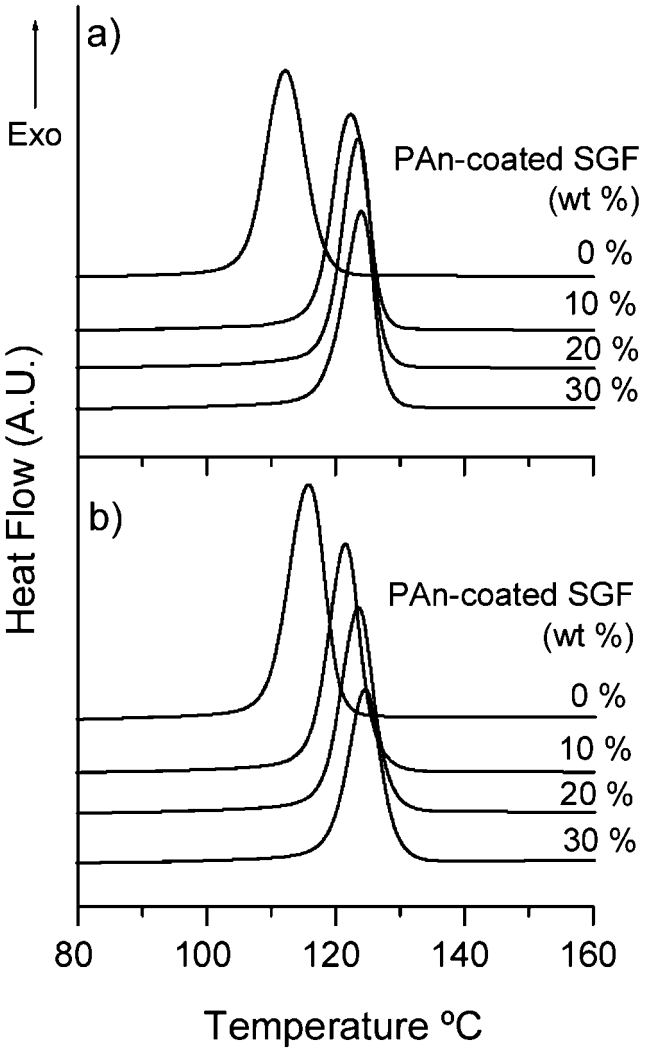

Figure 5 DSC scans of the composites at different loadings of PAn-coated SGF prepared by blending with: (a) iPP and (b) iPP/PP-*g*MA blend.

(130), (111), and the overlapped (131) and (041) reflections of the α phase of iPP.[37] However, after addition of the PAn-coated SGF, the ratio between the peaks corresponding to the (110) and (040) reflection planes change, as shown for composites of iPP and iPP/PP-*g*MA containing 30 wt % of PAn-coated SGF (Fig. 6, curves c and d, respectively). This change can be attributed to different orientation of the polymer chains near the surface of the composite,[38] which may have been induced by the press molding process in presence of the PAn-coated SGF.

Morphology and mechanical properties

The SEM micrograph of the fracture surface of the composite of iPP with 30% of PAn-coated SGF is shown in Figure 7(a). The large number of debonded fibers evidences the weak interaction between the fibers and the iPP. During the fracture, pullout of the fibers occurs, indicating that the stress is not transferred to the reinforcing fibers. However most of the fibers are still coated, most probably with PAn, because iPP has poor adhesion to glass fibers and the fracture of iPP/glass fiber composites shows mainly clean pulled-out glass fibers.[1] In the Figure 7(b), the surface fracture of the iPP/PP-*g*MA sample containing 30 wt % of PAn-coated SGF is shown. Both the wetting and dispersion of the fibers improved drastically upon addition of the PP-*g*MA, in part due to the lower melt viscosity of PP-*g*MA. On the other hand, the higher polar nature of the adhesion promoter makes the matrix more compatible with PAn compared to iPP, resulting in an increase in the adhesion between the fiber and the matrix in iPP/PP-*g*MA composites. In consequence, the fracture mechanism now involves fiber breakage, indicating that the stress was efficiently transferred to the reinforcement.

The Young's moduli of the composites are shown in Figure 8(a). A linear increment upon addition of the PAn-coated SGF is displayed for both types of composites. We calculated the efficiency factor values for both set of composites using the Krenchel's law,[39] where V is the volume fraction and E the modulus, and the subscripts f and m refer to the fiber and the polymer matrix, respectively, and η is the Krenchel's efficiency factor.

$$E = \eta E_f V_f + E_m V_m \quad (1)$$

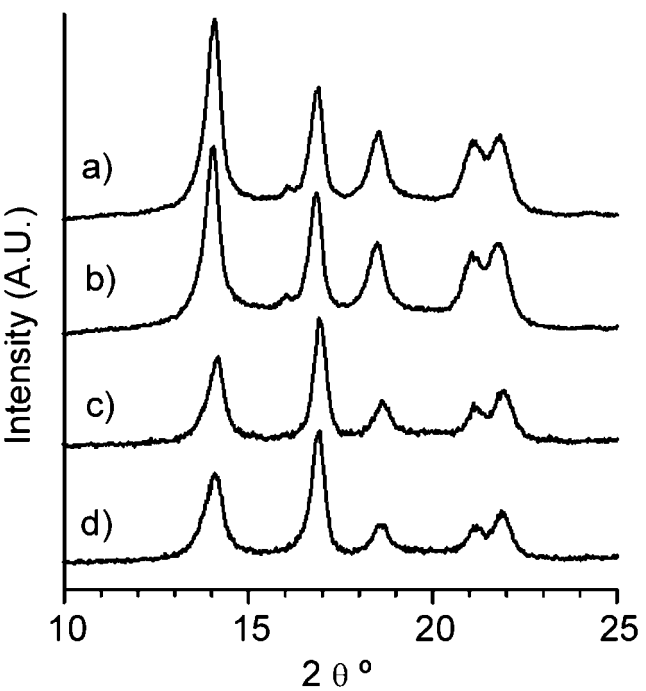

Figure 6 WAXD patterns of (a) iPP, (b) iPP/PP-*g*MA blend, (c) iPP with 30 wt % of PAn-coated SGF, and (d) iPP/PP-*g*MA blend with 30 wt % of PAn-coated SGF.

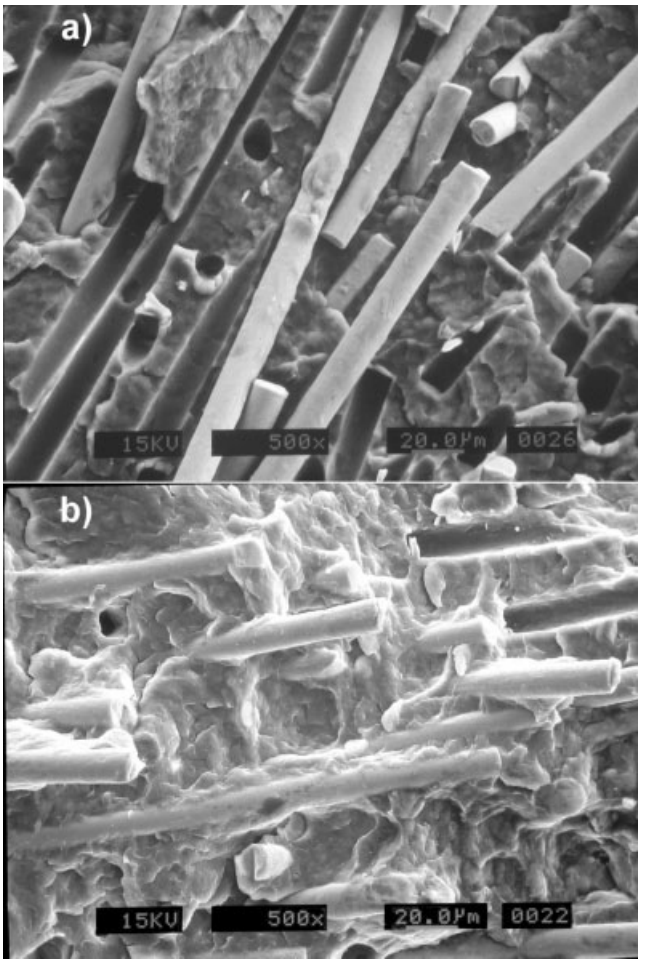

Figure 7 Typical fracture surfaces of compression molded composites: (a) iPP with 30 wt % of PAn-coated SGF and (b) iPP/PP-*g*MA blend with 30 wt % of PAn-coated SGF.

The efficiency factor depends on the fiber length and orientation and fiber-matrix interfacial adhesion, but since the addition of the PP-*g*MA affects mainly this last parameter; thus we can ascribe the change of the efficiency factor to the presence of the adhesion promoter. The efficiency factor calculated using the eq. (1) for iPP/PAn-coated SGF composites was 0.16 and for the iPP/PP-*g*MA/PAn-coated SGF composites was 0.33. The twofold increment when PP-*g*MA was used indicates the improvement of the fiber-matrix interfacial adhesion, increasing the modulus from 1.9 to 4.5 GPa at 30 wt % of PAn-coated SGF. The tensile strength in both set of composites showed a reduction after addition of the PAn-coated SGF due to the effect of interfacial flaws [Fig. 8(b)]. This is because tensile strength is measured after irreversible deformation of the sample and fiber-matrix void formation, and thus is less sensitive to reinforcement as compared to Young's modulus.

Whereas interaction between PAn-coated SGF and iPP is mainly mechanical because of the high roughness of the fiber [Fig. 2(b)], several chemical interactions could arise between the PAn-coated SGF and the PP-*g*MA. The amino end-groups of the PAn can react with the maleic anhydride groups of the PP-*g*MA, producing an amide that under high temperature can further react by condensation, originating an imide group,[40] as shown in Figure 9. This covalent bonding between the PAn and the polymer matrix would explain in some extent the increment of the interfacial adhesion. In addition, due to partial debonding of the PAn-coated SGF due to abrasion or shear stress during melt processing, the PP-*g*MA can react either with the silanol groups[27] (produced by the acid treatment of the fiber) or with the secondary amine groups of the silane on the exposed surface of the glass fiber.

Electrical properties

PP-g-MA was an effective adhesion promoter improving the Young's module of composites of iPP

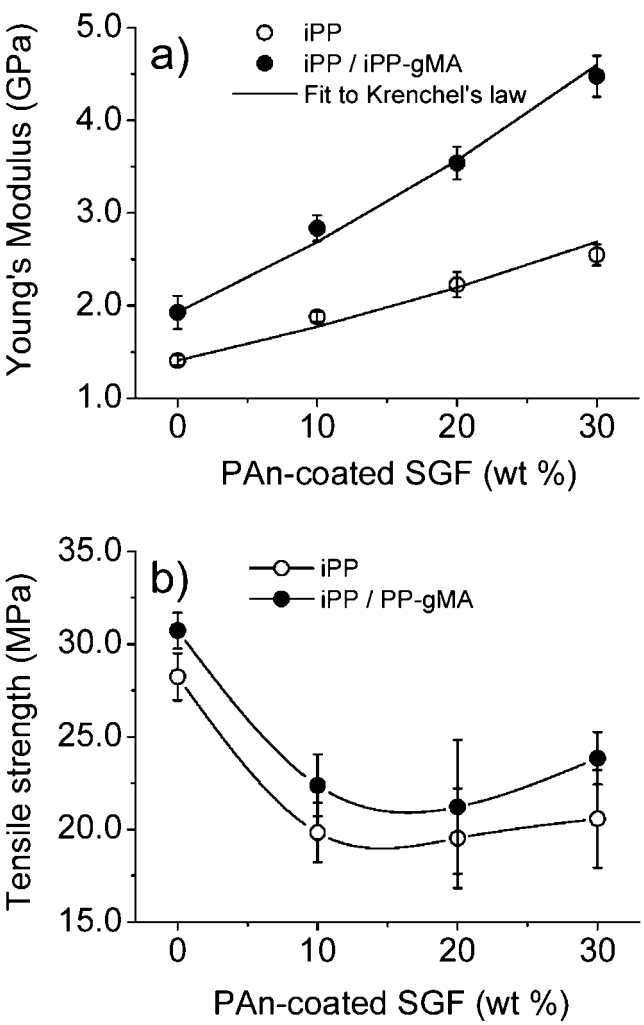

Figure 8 (a) Young's modulus and (b) tensile strength of the composites of iPP and iPP/PP-*g*MA as a function of PAn-coated SGF loading.

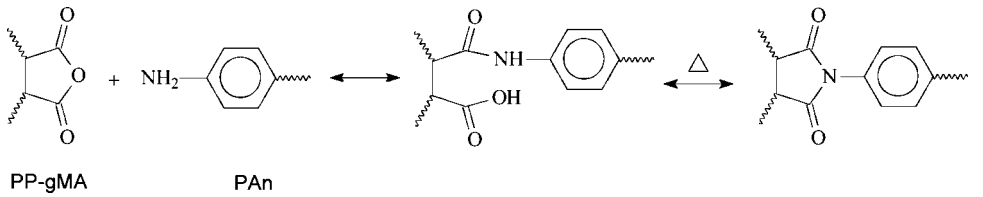

Figure 9 Proposed reaction between PAn end-groups and maleic anhydride groups.

with PAn-coated SGF; however its effect on electrical conductivity should be analyzed. The conductivity of the composites versus the amount of PAn-coated SGF is shown in Figure 10. The composite of iPP with PAn-coated SGF increments its electrical conductivity by three orders as the amount of fiber is increased from 20 to 30 wt %, indicating a percolation phenomena, whereas the composite containing PP-*g*MA shows only a slight increment. This is due to PAn-coated SGF encapsulation after addition of the adhesion promoter, and is supported by SEM observations [Fig. 7(b)]. Similar electrical conductivity behavior has been obtained in PP–stainless steel fiber composites[41] and ethylene vinyl acetate copolymer/copoliamide/PAn ternary blends[42] when adhesion promoters were added. All the composites have similar electrical conductivity values, in the 10^{-13} to 10^{-12} S/cm order, regardless of the measuring direction, except for the composite of iPP with 30 wt % of PAn-coated SGF, that has a conductivity three orders of magnitude higher when measured perpendicular to the compression direction. This is because fiber orientation is induced near the surface by the compression molding, helping to achieve the percolation along the plane of compression, producing an anisotropic electrically conductive composite at lower concentration that those containing random oriented fibers.[12] Addition of more than 30 wt % of PAn-coated SGF not necessarily would lead to an increase of electrical conductivity because of the increase of fiber breakage and abrasion. Composites of electrically conductive metallic fibers and thermoplastics often achieve the percolation at 6% to 10% volume fraction,[13,41] but in our case, the resulting electrical conductivity of the iPP/PAn-coated SGF is lower than the expected, indicating that partial debonding of the PAn coating took place during processing. This is further supported by optical microscopy images [Fig. 3(b)]. Nevertheless, the electrical conductivity reached at 30 wt % of loading was in the range of electrostatic discharge applications using a very low amount of PAn in the composite (~1.2 wt % of PAn). To further improve this composite, the addition of low-viscosity melt-processable PAn complex may increase the electrical conductivity by acting as a bridge between the electrically conductive segments of the individual fibers, as it does in carbon fiber/melt-processable PAn composites,[4] and by reducing the debonding of the PAn-coated SGF. This work demonstrates that PAn-coated SGF is a potential application of this conductive polymer; however the processing conditions may be optimized to reduce the coating debonding of the glass fiber during melt processing and to improve the electrical and mechanical properties of the composite.

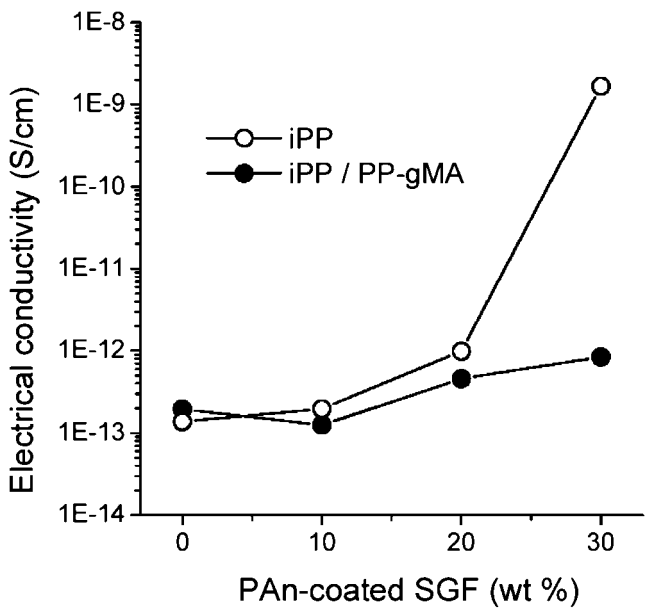

Figure 10 Electrical conductivity as a function of PAn-coated SGF loading for iPP and iPP/PP-*g*MA composites.

CONCLUSIONS

PAn-coated SGF was prepared in a novel unstirred reactor that overcomes problems with large unstirred aniline polymerizations, such as autoacceleration and increase of the reaction media temperature. A high fiber/liquor weight ratio (1 : 3) was achieved, while breakage of glass fiber and abrasion of the coating was avoided because of fiber immobilization. PAn-coated SGF showed a strong nucleating activity towards iPP, resulting in a shift of the crystallization temperature up to 12°C. Polarized light microscopy showed the formation of transcrystalline zones on the PAn-coated SGF vicinity, and X-ray diffraction patterns indicates that the crystalline phase of both

matrix and transcrystalline zones are α-type. Addition of PAn-coated SGF incremented the Young's modulus of the composites. Maleated PP proved to be an effective adhesion promoter, increasing both dispersion and wetting of the fibers, but affected negatively the electrical conductivity of the composites due to fiber encapsulation. A reaction between the maleic groups of the adhesion promoter and the terminal amino groups of PAn was proposed to explain the improvement in interfacial adhesion. The electrical conductivity reached with a very low fraction of PAn (30 wt % of PAn-coated SGF, equivalent to 1.2 wt % of PAn) and is in the range of electrostatic discharge applications.

Blanca Huerta, Sandra Peregrina, and Esmeralda Saucedo are acknowledged for thermal analyses, mechanical properties evaluation, and SEM images, respectively. Edgar Amaro is acknowledged for electrical conductivity measurements and R. Cruz-Silva thanks Prof. Felipe Avalos for helpful discussion.

References

1. Taipalus, R.; Harmia, T.; Friedrich, K. Appl Compos Mater 1999, 6, 167.
2. Jia, W.; Tchoudakov, R.; Segal, E.; Narkis, M.; Siegmann, A. J Appl Polym Sci 2004, 91, 1329.
3. Faez, R.; Martin, I. M.; de Paoli M.-A.; Rezende M. C. J Appl Polym Sci 2002, 83, 1568.
4. Taipalus, R.; Harmia, T.; Friedrich, K. Polym Compos 2000, 21, 396.
5. Flandin, L.; Bidan, G.; Brechet, Y.; Cavaillé, J. Y. Polym Compos 2000, 21, 165.
6. Jia, W.; Tchoudakov, R.; Segal, E.; Joseph, R.; Narkis, M.; Siegmann, A. Synth Met 2003, 132, 269.
7. Barra, G. M. O.; Jacques, L. B.; Oréfice, R. L.; Carneiro, J. R. G. Eur Polym J 2004, 40, 2017.
8. Macdiarmid, A. G. Curr Appl Phys 2001, 1, 269.
9. Ikkala, O. T.; Laakso, J.; Väkiparta, K.; Virtanen, E.; Ruohonen, H.; Järvinen, H.; Taka, T.; Passiniemi, P.; Österholm, J.-E.; Cao, Y.; Smith, P.; Heeger, A. J. Synth Met 1995, 69, 97.
10. Schacklette, L. W.; Han, C. C.; Luly, M. H. Synth Met 1993, 57, 3532.
11. Kirkpatrick, S. Rev Mod Phys 1973, 45, 574.
12. Balberg, I.; Binenbaum, N.; Wagner, N. Phys Rev Lett 1984, 52, 1465.
13. Xie, Q. Eur Polym J 2004, 40, 323.
14. Weber, M.; Kamal, M. R. Polym Compos 1997, 18, 711.
15. Sumita, M.; Sakata, K.; Hayakawa, Y.; Asai, S.; Miyasaka K.; Tanemura, M. Colloid Polym Sci 1992, 270, 134.
16. Levon, K.; Margolina, A.; Patashinsky, A. Z. Macromolecules 1993, 26, 4061.
17. Genetti, W. B.; Yuan, W. L.; Grady, B. P.; O'rea, E. A.; Lai, C. L.; Glatzhofer, D. T. J Mater Sci 1998, 33, 3085.
18. Gregory, R. V.; Kimbrell, W. C.; Kuhn, H. H. Synth Met 1989, 28, 823.
19. Dong, H.; Prasad, S.; Nyame, V.; Jones, W. E. Chem Mater 2004, 16, 371.
20. Kim, S. H.; Seong, J. H.; Oh, K. W. J Appl Polym Sci 2002, 83, 2245.
21. Anbarasan, R.; Jayaseharan, J.; Sudha, M.; Gopalan, A. J Appl Polym Sci 2003, 90, 3827.
22. Lekpittaya, P.; Yanumet, N.; Grady, B. P.; O'rear, E. A. J Appl Polym Sci 2004, 92, 2629.
23. Geetha, S.; Kannan, K.; Kumar, S.; Trivedi, D. C. J Appl Polym Sci 2005, 96, 2316.
24. Wu, C. G.; Chen, J. Y. Chem Mater 1997, 9, 399.
25. Wu, C.-G.; Yeh, Y.-R.; Chen, J.-Y.; Chiou, Y.-H. Polymer 2001, 42, 2877.
26. Li, Z. F.; Ruckenstein, E. J Colloid Interface Sci 2002, 251, 343.
27. Bikiaris, D.; Matzinos, P.; Larena, A.; Flaris, V.; Paayiotou, C. J Appl Polym Sci 2001, 81, 701.
28. Bettini, S. H. P.; Agnelli, J. A. M. Polymer Test 2000, 19, 3.
29. Lu, X.; Ng, H. Y.; Xu, J.; He, C. Synth Met 2002, 128, 167.
30. Brandup, J.; Immergut, E. H. Polymer Handbook; Wiley: New York, 1988; Vol. 3, Chapter 8.
31. Riede, A.; Helmstedt, M.; Riede, V.; Zemek, J.; Stejskal, J. Langmuir 2000, 16, 6240.
32. Cruz-Silva, R.; Romero-Garcia, J.; Angulo-Sanchez, J. L. Mater Sci 2005, 40, 5107.
33. Bogoeva-Gaceva, G.; Janevski, A.; Mader, E. Polymer 2001, 42, 4409.
34. Hristov, V.; Vasileva, S. Macromol Mater Eng 2003, 288, 798.
35. Dean, D. M.; Register, R. A. J Polym Sci Part B: Polym Phys 1998, 36, 2821.
36. Xie, H.-Q.; Zhang, S.; Xie, D. J Appl Polym Sci 2005, 96, 1414.
37. Thomann, R.; Wang, C.; Kressler, J.; Mülhaupt, R. Macromolecules 1996, 29, 8425.
38. Cerrada, M. L.; Prieto, O.; Pereña, J. M.; Benavente, R.; Perez, E. Rev Plast Mod 2002, 84, 168.
39. Krenchel, H. Fibre Reinforcement; Akademisk Forlag: Copenhagen, 1964.
40. Major, J. S.; Blanchard, G. J. Chem Mater 2002, 14, 2567.
41. Tan, S.-T.; Zhang, M.-Q.; Rong, M.-Z.; Zeng, H.-M. Polym Compos 1999, 20, 406.
42. Cooper, H.; Segal, E.; Srebnik, S.; Tchoudakov, R.; Narkis, M.; Siegmann, A. J Appl Polym Sci 2006, 101, 110.